AGU PUBLICATIONS

Geophysical Research Letters

RESEARCH LETTER
10.1002/2016GL068015

Key Points:
- Late Holocene RSL rise rates are compared to GPS vertical rates along the Atlantic Coast of North America
- Holocene RSL data are used to separate long-term GIA-induced displacement from the modern rate
- Differences between geologic and GPS rates occur in areas of excessive groundwater extraction

Supporting Information:
- Supporting Information S1
- Table S1
- Table S2

Correspondence to:
M. A. Karegar,
makan.karegar@gmail.com

Citation:
Karegar, M. A., T. H. Dixon, and S. E. Engelhart (2016), Subsidence along the Atlantic Coast of North America: Insights from GPS and late Holocene relative sea level data, *Geophys. Res. Lett.*, *43*, 3126–3133, doi:10.1002/2016GL068015.

Received 29 JAN 2016
Accepted 15 MAR 2016
Accepted article online 17 MAR 2016
Published online 2 APR 2016

Subsidence along the Atlantic Coast of North America: Insights from GPS and late Holocene relative sea level data

Makan A. Karegar[1], Timothy H. Dixon[1], and Simon E. Engelhart[2]

[1]School of Geosciences, University of South Florida, Tampa, Florida, USA, [2]Department of Geosciences, University of Rhode Island, Kingston, Rhode Island, USA

Abstract The Atlantic Coast of North America is increasingly affected by flooding associated with tropical and extratropical storms, exacerbated by the combined effects of accelerated sea-level rise and land subsidence. The region includes the collapsing forebulge of the Laurentide Ice Sheet. High-quality records of late Holocene relative sea-level (RSL) rise are now available, allowing separation of long-term glacial isostatic adjustment-induced displacement from modern vertical displacement measured by GPS. We compare geological records of late Holocene RSL to present-day vertical rates from GPS. For many coastal areas there is no significant difference between these independent data. Exceptions occur in areas of recent excessive groundwater extraction, between Virginia (38°N) and South Carolina (32.5°N). The present-day subsidence rates in these areas are approximately double the long-term geologic rates, which has important implications for flood mitigation. Tide gauge records, therefore, should be used with caution for studying sea-level rise in this region.

1. Introduction

Eastern North America is a passive continental margin. Most of this margin is experiencing spatially variable, long-term vertical motion due to glacial isostatic adjustment (GIA), a viscoelastic response of the Earth's crust and mantle to retreat of the Laurentide Ice Sheet since the last glacial maximum ~20,000 years ago [e.g., *Peltier*, 2004]. GIA drives land uplift in areas under the former Laurentide Ice Sheet and land subsidence in peripheral areas as the forebulge beyond the former ice sheet margin collapses. Subsidence along parts of the Atlantic Coast constitutes the largest-amplitude proglacial forebulge collapse on Earth. Although GIA is the dominant contributor to vertical land motion in this region, other processes also contribute to crustal movement here. Groundwater withdrawal and recharge induces spatially and temporally variable vertical motion in the Atlantic coastal plain [*Depaul et al.*, 2008; *Boon et al.*, 2010]. Sediment loading [*Calais et al.*, 2010], sediment compaction [*Miller et al.*, 2013], topographic relaxation of the slowly eroding Appalachians [*Ghosh et al.*, 2009], ridge push generated by cooling of the oceanic portion of the North American plate [*Zoback*, 1992], mantle flow-induced dynamic topography [*Rovere et al.*, 2015], and in-plane stress-induced deformation [*Cloetingh et al.*, 1985; *Karner*, 1986] are additional active processes that may also contribute to vertical motion in this "passive" margin environment. Since coastal locations are impacted by flooding from tropical and extratropical storms, the combined effects of accelerating sea-level rise and land subsidence need to be considered in long-term flood mitigation and planning [e.g., *Dixon et al.*, 2006; *Ezer and Atkinson*, 2014].

Vertical land motion has been measured with continuous GPS stations across the North American plate interior [*Sella et al.*, 2002; *Park et al.*, 2002; *Calais et al.*, 2006; *Sella et al.*, 2007; *Argus and Peltier*, 2010; *Peltier et al.*, 2015] and along the coastal plain near tide gauges [*Snay et al.*, 2007; *Bouin and Wöppelmann*, 2010; *Santamaría-Gómez et al.*, 2012]. Along the eastern seaboard, these studies have been limited by the number and time span of available data [*Peltier et al.*, 2015]. *Engelhart et al.* [2009] and *Kemp et al.* [2014] compared late Holocene relative sea level (RSL) data with available GPS vertical rates calculated by *Snay et al.* [2007] and *Sella et al.* [2007] and found significant discrepancies. Some of these discrepancies can be attributed to the short GPS time series then available. Other discrepancies may reflect the influence of time-variable groundwater extraction and recharge. New GPS data based on longer time series (average record length of 8.5 years) and additional stations (~190 new sites) are now available, allowing substantial refinement of the present-day vertical velocity field. Here we investigate vertical land motion in the central part of eastern

coastal North America, based on 216 continuous GPS sites between New Brunswick, Canada, and southern Florida, U.S., using all available data to January 2015. We compare these data to high-quality geological records of Holocene RSL describing vertical land motion in the region from 4 ka B.P. to 1900 A.D. We then discuss the major processes affecting the present-day vertical velocity field.

2. Data and Analysis Methods

2.1. GPS

The GPS stations analyzed here have nearly continuous observations, ranging from 4 to 18 years. More than 70 stations have recorded data for longer than 10 years. The raw GPS data were processed using the software package GIPSY/OASIS II (V. 6.2) of the Jet Propulsion Laboratory (JPL) and the precise point positioning technique (see supporting information Text S1). The nonfiducial daily position time series are transformed into the IGb08 reference frame [*Rebischung et al*., 2012] using JPL's X files, a seven-parameter transformation.

It has long been recognized that the formal errors of GPS displacement time series based on a white noise approximation underestimate the uncertainty of site velocity [e.g., *Mao et al*., 1999]. Time-correlated (colored) noise can be estimated using spectral analysis and maximum likelihood estimation [*Mao et al*., 1999; *Williams*, 2008; *Bos et al*., 2008]. Here we estimate the vertical rate uncertainties using the Allan variance of rate technique of *Hackl et al*. [2011] as described in *Karegar et al*. [2015].

2.2. Late Holocene Relative Sea Level Database

Reconstructions of late Holocene (last 4000 years) RSL have recently been compiled to create a database defining vertical land motion along the Atlantic Coast of the U.S. [*Engelhart and Horton*, 2012; *Kemp et al*., 2014; *Nikitina et al*., 2015]. The methodology is described in the *Handbook of Sea-Level Research* [*Shennan et al*., 2015] and recent publications [*Engelhart et al*., 2009; *Engelhart and Horton*, 2012; *Hijma et al*., 2015]. These data assume that late Holocene ice equivalent meltwater input is minimal from 4 ka B.P. until 1900 A.D.; therefore, RSL trends are an estimate of spatially variable land motion primarily dominated by GIA. A recent study shows global eustatic sea-level rise of $\leq$1 m from 4.2 ka B.P. to 1900 A.D [*Lambeck et al*., 2014]. Ocean syphoning (migration of water into subsiding peripheral bulges) is also known to affect late Holocene sea-level rise [*Mitrovica and Milne*, 2002]. Late Holocene RSL data suggest a tectonic uplift rate of $\sim 0.2 \pm 0.2$ mm yr^{-1} along the Cape Fear Arch (southeastern United States) [*van de Plassche et al*., 2014], but along much of the passive Atlantic Coast of North America, the tectonic contribution to RSL data is assumed to be negligible. The effects of natural compaction of Holocene sediment are minimized by using basal peat samples [*Engelhart et al*., 2009]. Compaction of the underlying (pre-Holocene) strata is believed to occur at low rates ($<$0.1 mm yr^{-1}) [*Kooi and de Vries*, 1998; *Kominz et al*., 2008; *Hayden et al*., 2008; *Horton et al*., 2013; *Miller et al*., 2013]. *Engelhart and Horton* [2012] recalculated rates of RSL change for 16 regions (from Maine to South Carolina; see Figure 1) for the last 4 ka after removing RSL change since 1900 A.D. based on measurements from the nearest reliable tide gauge. These regions are classified based on data availability, distance from the center of the former Laurentide Ice Sheet, and susceptibility to Holocene sediment compaction. We expand/modify the *Engelhart et al*. [2009] data to reflect the availability of new data and to incorporate data from a site in southern Canada. A RSL history produced for the southern New Brunswick coast (Canada) at Little Dipper Harbour (45.1°N, 66.4°W) shows that late Holocene RSL at this location has been about 1 m/1000 years [*Gehrels et al*., 2004], i.e., $\sim$1 mm yr^{-1} subsidence rate. *Nikitina et al*. [2015] produce a new RSL record covering the last 2200 years in Delaware Bay (39°N, 75°W). They showed that *Engelhart et al*. [2009] overestimated the late Holocene RSL rate in the inner bay due to tidal range changes. *Kemp et al*. [2014] provides the RSL data from 2.5 ka to 1800 A.D. from the border of Georgia and northeastern Florida.

Given ongoing mantle relaxation, there is a possibility that late Holocene RSL rates are biased by record length (lower rates for later periods). *Engelhart and Horton* [2012] compared linear rates of RSL rise from 2 ka B.P. to 1900 A.D. with linear rates from 4 ka B.P. to 1900 A.D. in 11 regions with sufficient data for both time periods. Within uncertainties, similar rates were obtained for the two periods. Supporting information Text S3 discusses a possible exception.

Uncertainties in the late Holocene RSL rates are derived from propagation of errors and depend on type of coring equipment, techniques of depth measurement, natural compaction of sediment during penetration, and error associated with the leveling of the sample with respect to the North American Vertical

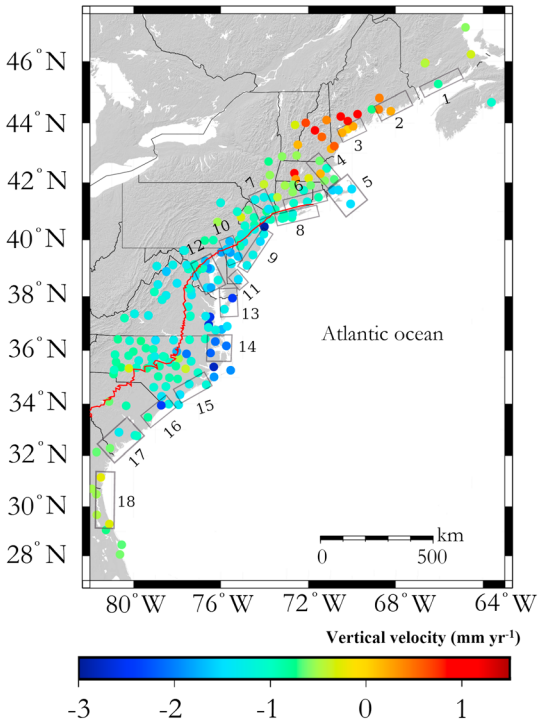

Figure 1. Map showing the location of GPS sites used in this study and 18 regions for which the late Holocene relative sea-level rise rate is known (region 1, *Gehrels et al.* [2004]; regions 2–17, *Engelhart et al.* [2009], *Engelhart and Horton* [2012], and *Nikitina et al.* [2015]; region 18, *Kemp et al.* [2014]). GPS and geologic rates for each region are detailed in supporting information Table S2. Red line shows the Fall Line, a boundary between compressible coastal plain sediments and incompressible bedrock of the Piedmont Province [*Meng and Harsh*, 1988]. Circle color indicates decadal average vertical land motion in IGb08 reference frame.

Datum of 1988 [see *Engelhart et al.*, 2009; *Engelhart and Horton*, 2012]. Effects of eustatic sea-level rise could also overestimate the vertical land motion from RSL data (<0.2 mm yr^{-1}) [*Lambeck et al.*, 2014].

3. Results

Our GPS analysis gives a present-day snapshot of vertical land motion at 216 sites along the East Coast of North America with an uncertainty of order 0.5 mm yr^{-1} or better (Figure 1 and supporting information Table S1). Subsidence rates of <1 mm yr^{-1} occur in New Brunswick, Canada, along the shoreline, transitioning to uplift rates of <1 mm yr^{-1} from Maine (45°N) to New Hampshire (43°N). All stations from New Hampshire to mid-Florida (28°N) show subsidence rates of <3 mm yr^{-1}. The highest subsidence rates concentrate in a coastal region from northern Delaware and Maryland (~40°N) to the northern part of North Carolina (~35°N) (mean ~1.5 mm yr^{-1}, up to ~3 mm yr^{-1}).

The surface vertical velocities defined by GPS are compared to the rates of late Holocene RSL rise in Figure 2a and supporting information Figure S1a. The pattern of subsidence obtained from the geologic data largely reflects ongoing GIA, including collapse of the proglacial forebulge. The GPS data exhibit a similar pattern, with exceptions discussed below. The GPS and geologic data indicate that the highest rates of subsidence due to forebulge collapse (1.3–1.5 mm yr^{-1}) extend from New Jersey (region 9, ~39°N) south to the Chesapeake Bay (region 13, ~ 37°N). To facilitate comparison, we also average rates from all GPS stations within specific areas where Holocene RSL rise data are available (18 boxes in Figure 1; Figure 2b, supporting information Figure S1b, and Table S2).

4. Discussion

Accurate determination of the forebulge location and amplitude is important for studies of RSL and flood mitigation. Recent findings show accelerated RSL along the coast north of Cape Hatteras (35.2°N), North Carolina, and significant variation of RSL rates along the U.S. eastern seaboard [*Boon et al.*, 2010; *Ezer and Corlett*, 2012; *Sallenger et al.*, 2012; *Kopp*, 2013]. Slowing of the Atlantic Meridional Overturning Circulation [*Sallenger et al.*, 2012; *Yang et al.*, 2016] and variations in the Gulf Stream location and intensity [*Ezer et al.*, 2013] have recently been identified as possible drivers of accelerated sea-level rise in this region. Our new data will be useful at separating the various contributions influencing present-day tide gauge RSL data, allowing better tests of these hypotheses.

There is a good agreement (within data uncertainty) between estimates of vertical land motion from GPS and geologic data along the Atlantic Coast of North America, except for two regions. Between 38°N and 32.5°N, present-day subsidence rates from GPS are approximately double the long-term geologic rates. In Maine (45°N–43°N), the GPS data show uplift whereas geologic data show subsidence (see supporting information Text S3).

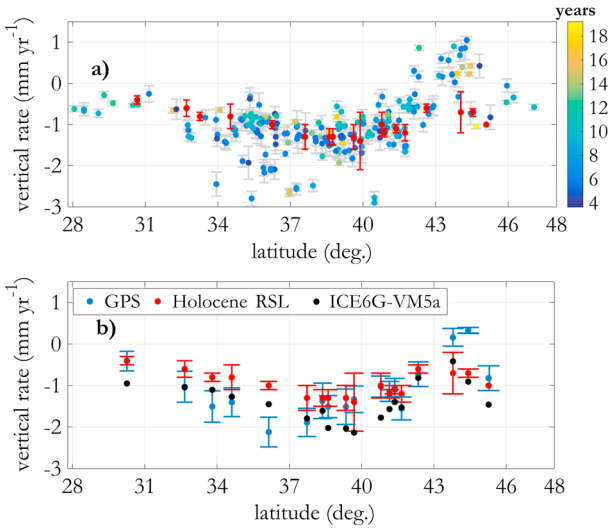

Figure 2. (a) Comparison of vertical motion as a function of latitude from GPS and geologic data. Color bar shows the length of time series for individual stations. (b) Spatially averaged GPS, geologic data, and GIA model ICE6G-VM5a (C). The GPS rate is averaged for all stations in the boxes shown in Figure 1.

At the regional scale, GPS rates reconcile with geologic rates in much of the mid-Atlantic (regions 1 and 4–12, 45.1°N and 43°N–38°N). The GPS and geologic rates also agree in Georgia and Florida (region 18; 31.5°N–29°N). Note that comparison of GPS and geologic rates is limited to 18 regions where late Holocene RSL data are available (Figure 1).

We use the latest GIA model, ICE6G-VM5a (C) [*Peltier et al.*, 2015], for comparison to the GPS and geologic data (Figure 2b). In ICE6G, the mantle viscosity VM5a model [*Peltier and Drummond*, 2008] is held fixed in the adjustment process, while the glaciation history (ICE5G-VM2) is refined to best fit selected GPS rate data in North America, Northwestern Europe/Eurasia, and Antarctica. We calculated the weighted root-mean-square (WRMS) of residuals (GPS or geologic rate minus the GIA model) to quantify the overall agreement between ICE6G-VM5a (C) and these other data. The WRMS of geologic rates relative to the GIA model (0.15 mm yr^{-1}) is smaller than the WRMS of GPS rates relative to the GIA model (0.66 mm yr^{-1}). The larger discrepancy between GPS and the GIA model may reflect larger uncertainties in GPS rates, inconsistency in the GPS and GIA model reference frames [e.g., *Kierulf et al.*, 2014], inappropriate selection of GPS sites to constrain the ICE6G-VM5a (C) GIA model, and non-GIA signals in our GPS data, e.g., signals related to groundwater fluctuations. Here we focus on this latter explanation.

The GPS subsidence rates decrease with distance away from the coastal plain and toward the center of mass loading of the Laurentide Ice Sheet (Figure 1). The geomorphic boundary (Fall Line, see Figure 1 and supporting information Figure S3a) that separates compressible coastal plain sediments (Cretaceous to Holocene unconsolidated sediments) and incompressible bedrock of the Piedmont Province closely corresponds to the boundary separating high subsidence rates (2–3 mm yr^{-1}) and low subsidence rates ($<$1 mm yr^{-1}). Subsidence of stations east of the Fall Line is also more variable than those of bedrock sites. Stations east of the Fall Line are likely affected by both groundwater fluctuations and natural sediment compaction. Groundwater extraction in excess of recharge reduces pore fluid pressure, leading to aquifer-related compaction and surface subsidence. Conversely, net groundwater recharge increases pore fluid pressure and can lead to uplift.

As noted earlier, the influence of shallow sediment compaction on Holocene RSL data is minimized through the use of basal peats. The agreement between GPS and Holocene RSL data in regions 9–12 (New Jersey to Virginia, 40°N–38°N, an area underlain by unconsolidated sediments) therefore implies that subsidence due to shallow sediment compactions is very small in the GPS data. This makes sense, because most of the GPS stations used in this study are installed on the top of buildings. Their monuments are building foundations that usually include concrete pilings, vertical structural columns driven to refusal, typically several meters or more in depth. Therefore, our GPS subsidence rates are not sensitive to compaction in the upper few meters of Holocene sediment. For purposes of flood mitigation and planning, the GPS rates should be considered minimum rates.

4.1. Effects of Groundwater Withdrawal

The GPS data reflect a combination of long-term deformation (e.g., from GIA, deep sediment compaction, and sedimentary isostatic adjustment) and short-term deformation (e.g., from groundwater withdrawal). The geologic rates of RSL (indicating long-term deformation) can be used to "correct" the GPS data to investigate recent changes to the vertical velocity field. This information may be useful to understand and predict future wetland loss and storm surge inundation, particularly in areas (e.g., north of Cape Hatteras) where accelerated sea-level rise has been observed and is associated with increased flooding [*Ezer and Atkinson*, 2014].

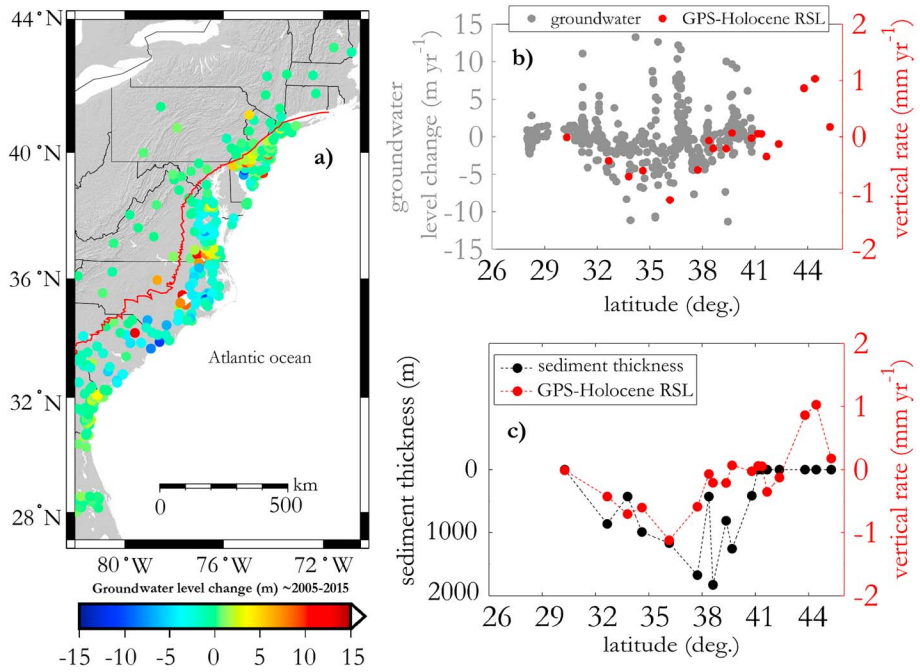

Figure 3. (a) Average trend in groundwater level since 2005. (b) GPS vertical velocities corrected for GIA and other long-term geologic effects (GPS rate minus late Holocene RSL rate calculated for each box shown in Figure 1) (red dots) and average trend in groundwater level changes (gray dots, east of Fall Line) versus latitude. (c) Corrected GPS vertical velocities (red dots) and sediment thickness [*Trapp and Meisler*, 1992] (black dots for each box) versus latitude.

Figure 3a shows the distribution of coastal groundwater monitoring wells with depth >100 m. We calculated the average trend in groundwater level since 2005, corresponding to the time span of most of the GPS observations. These data and other studies [e.g., *Konikow*, 2013; *Russo et al.*, 2015] demonstrate that the central and southern Atlantic coastal plain (Virginia and the Carolinas) are experiencing groundwater declines. We can test whether areas experiencing rapid modern subsidence correlate with areas of intense groundwater extraction, as follows. We subtract the geologic subsidence rate (which includes the GIA component) from the average GPS rate calculated for each box shown in Figure 1 to derive a residual rate ("GPS minus Holocene RSL" in Figure 3a and 3b). We then compare these residual rates with the average trend of groundwater level as a function of latitude (Figure 3b). In the central and southern Atlantic coastal plains (38°N–32°N), we observe a correlation between rapid subsidence and groundwater depletion, consistent with the idea that excessive groundwater extraction is driving rapid land subsidence in these regions. The short-term GPS subsidence rates are double the long-term geologic subsidence rates.

The Atlantic coastal plain is composed of a multilayered aquifer system underlain by a wedge of unconsolidated to semiconsolidated sedimentary rocks. The sedimentary wedge thickens eastward beneath the continental shelf, ranging from a featheredge near the Fall Line to about 3000 m at Cape Hatteras (35.2°N), North Carolina (supporting information Figure S3a). The relatively weak correlation between local GPS subsidence and local coastal plain thickness ($\rho = 0.40$; supporting information Figure S3b) implies that subsidence due to natural compaction of deep sediment and sedimentary isostatic loading, while present, is not the major process affecting these data. Both GPS and geologic subsidence rates include the effects of natural compaction of deep strata and sedimentary isostatic loading as well as GIA. These long-term effects are presumably eliminated from the GPS rates by subtracting the corresponding geologic rates. Figure 3c shows these "corrected" GPS subsidence rates, which better correlate with the thickness of underlying coastal plain sediments ($\rho = 0.54$; supporting information Figure S3c). A possible explanation is that regions underlain by thicker sediments are more susceptible to faster recent subsidence, perhaps due to groundwater extraction and aquifer compaction. Supporting information Figure S4 and Text S5 discuss possible correlations with population density and other indirect indicators of groundwater extraction rates.

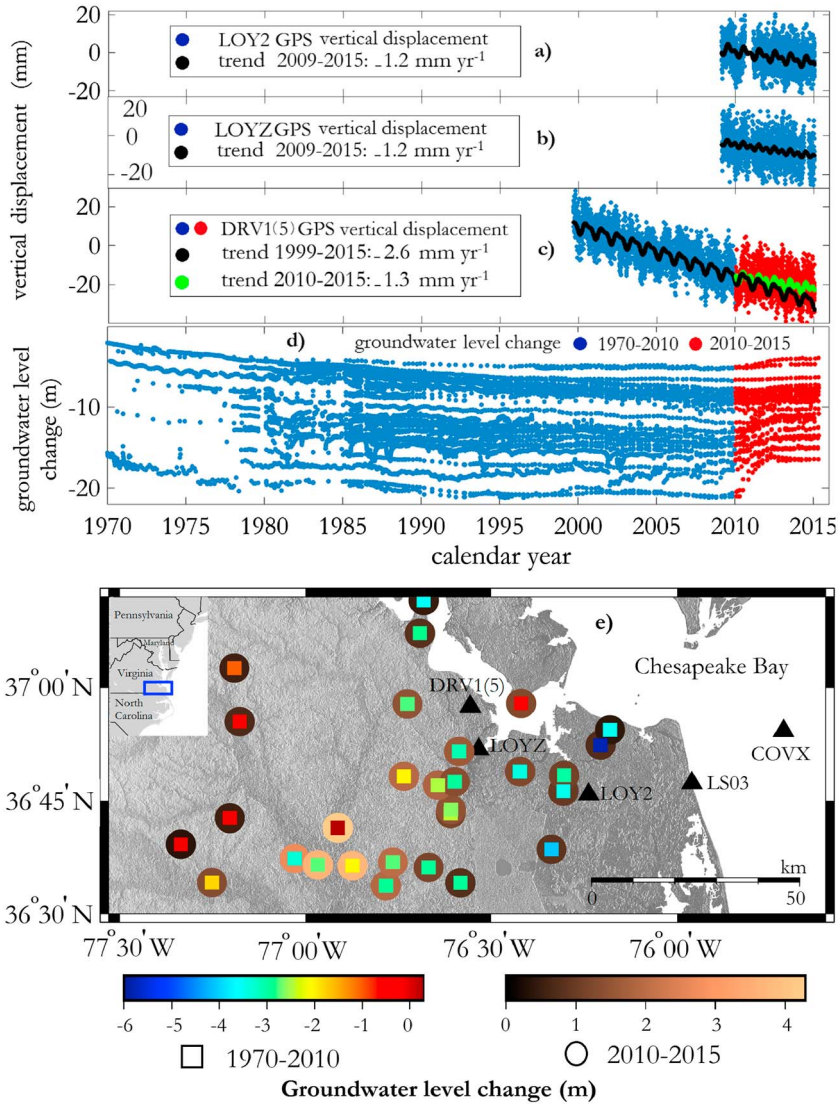

Figure 4. Vertical motion in south of Chesapeake Bay, Virginia, from GPS stations: (a) LOY2, (b) LOYZ, (c) DRV1 (5), and (d) time series of groundwater level change in south of Chesapeake Bay. (e) Location of groundwater monitoring wells (squares and circles) and GPS sites (black triangles) in southern Chesapeake Bay. Square colors indicate groundwater level decrease (1970 to 2010), while circle colors indicate groundwater level increase from 2010 to 2015.

The groundwater level in most of the southern Chesapeake Bay region (south of Virginia) declined from the early 1970s until the late 2000s in response to excessive withdrawal. However, from the late 2000s until the present (2015), the trend reversed, indicating groundwater recharge (Figure 4). In unconsolidated sediments, aquifer recharge increases pore fluid pressure and results in surface uplift. The longest GPS time series in the southern Chesapeake Bay region spans September 1999 to January 2015 at site DRV1 (DRV5 after June 2006). Figure 4c shows vertical displacement at this site, where land subsided at 2.6 mm yr^{-1} from 1999 to 2010 and at 1.3 mm yr^{-1} (essentially the GIA rate) from 2010 to 2015. The observed displacements correlate with the abrupt increase in groundwater levels at nearby wells after about 2010 (Figure 4). The subsidence rate of 1.3 mm yr^{-1} for the period 2010–2015 at DRV1(5) agrees with subsidence rates observed at nearby GPS stations with shorter observational period (2009–2015) and the long-term geologic rate of 1.3 mm yr^{-1} for region 12. Subsidence prior to 2010 in southern Chesapeake Bay was double the geologic rate, while subsidence after 2010 occurred at the geologic rate. Tide gauge records here will need to be corrected for these effects in order to investigate recent sea-level changes. Our result also suggests that recent changes in groundwater management have been effective at reducing aquifer compaction.

In summary, for the region from Virginia to South Carolina (38°N to 32.5°N) approximately 50% of present-day land subsidence is related to groundwater depletion and consequent aquifer compaction.

5. Conclusions

Installation and operation of more than 130 continuous GPS stations in eastern coastal North America since 2006 represents a significant improvement in our ability to precisely define present-day vertical land motions in this region, improving our ability to understand and predict RSL variations and long-term flood hazard [e.g., *Bouin and Wöppelmann*, 2010].

Comparison of present-day vertical land motions estimated from GPS with rates of late Holocene RSL rise determined geologically indicates substantial agreement in most areas.

The geologic rate of RSL change provides an independent constraint to separate the long-term GIA-induced displacement (average motion over the past 2–4 ka) from the GPS vertical displacement (average over one to two decades). The present-day subsidence rates measured by GPS between Virginia (38°N) and South Carolina (32.5°N) are approximately double the long-term geologic rates, most likely reflecting recent groundwater depletion. Differences between the geologic and geodetic data are useful for understanding some of the human impacts in the coastal plain and for flood mitigation. For example, parts of the coastal plain (north of Cape Hatteras, North Carolina, 35.2°N) are susceptible to frequent minor to moderate storm-related flooding due to the combined effects of accelerated sea-level rise and land subsidence. Knowledge of present-day subsidence can help mitigate coastal land loss and predict future storm surge inundation.

Acknowledgments

This work was supported by NASA grant NNX14AQ16G to T.H.D. and M.A.K., NSF grant OCE-1458903, the U.S. Department of Agriculture National Institute of Food and Agriculture, Hatch funding, and the Rhode Island Agricultural Experiment Station grant RI0015 H104 contribution 5442 to S.E.E. The GPS data used in this study are archived at CORS (http://www.ngs.noaa.gov/CORS/), SOPAC (https://igscb.jpl.nasa.gov/components/dcnav/sopac_rinex.html), UNAVCO (https://www.unavco.org/data/gps-gnss/ftp/ftp.html), and Maine Technical Source (http://www.mainetechnical.com/c6/gps-data-post-processing-c7.html). The groundwater level data are available from the U.S. Geological Survey groundwater information page (http://waterdata.usgs.gov/nwis), North Carolina Division of Water Source (http://www.ncwater.org/?page=20), and South Carolina Department of Natural Resources (http://www.dnr.sc.gov/water/hydro/groundwater/groundwater.html). The GIA model ICE6G-VM5a (C) is available from the University of Toronto database (http://www.atmosp.physics.utoronto.ca/~peltier/data.php). We thank Torbjörn E. Törnqvist and Michael S. Steckler, whose thoughtful comments greatly improved the manuscript. We thank Torbjörn E. Törnqvist and Mead A. Allison for bringing the authors together at a stimulating workshop on coastal subsidence. This paper is a contribution to IGCP Project 639.

References

Argus, D. F., and W. R. Peltier (2010), Constraining models of postglacial rebound using space geodesy: A detailed assessment of model ICE-5G (VM2) and its relatives, *Geophys. J. Int.*, *181*(2), 697–723.

Boon, J. D., J. M. Brubaker, and D. R. Forrest (2010), Chesapeake Bay land subsidence and sea level change App. Mar. Sci. and Ocean Eng., Rep., 425, 1-73.

Bos, M. S., R. M. S. Fernandes, S. D. P. Williams, and L. Bastos (2008), Fast error analysis of continuous GPS observations, *J. Geod.*, *82*(3), 157–166.

Bouin, M. N., and G. Wöppelmann (2010), Land motion estimates from GPS at tide gauges: A geophysical evaluation, *Geophys. J. Int.*, *180*(1), 193–209.

Calais, E., J. Y. Han, C. DeMets, and J. M. Nocquet (2006), Deformation of the North American plate interior from a decade of continuous GPS measurements, *J. Geophys. Res.*, *111*, B06402, doi:10.1029/2005JB004253.

Calais, E., A. M. Freed, R. Van Arsdale, and S. Stein (2010), Triggering of New Madrid seismicity by late-Pleistocene erosion, *Nature*, *466*(7306), 608–611.

Cloetingh, S., H. McQueen, and K. Lambeck (1985), On a tectonic mechanism for regional sealevel variations, *Earth Planet. Sci. Lett.*, *75*(2), 157–166.

DePaul, V. T., D. E. Rice, and O. S. Zapecza (2008), Water-level changes in aquifers of the Atlantic coastal plain, predevelopment to 2000, *U.S. Geol. Surv. Sci. Invest. Rep., 2007–5247*, 1–88.

Dixon, T. H., F. Amelung, A. Ferretti, F. Novali, F. Rocca, R. Dokka, G. Sella, S. W. Kim, S. Wdowinski, and D. Whitman (2006), Space geodesy: Subsidence and flooding in New Orleans, *Nature*, *441*(7093), 587–588.

Engelhart, S. E., and B. P. Horton (2012), Holocene sea level database for the Atlantic Coast of the United States, *Quat. Sci. Rev.*, *54*, 12–25.

Engelhart, S. E., B. P. Horton, B. C. Douglas, W. R. Peltier, and T. E. Törnqvist (2009), Spatial variability of late Holocene and 20th century sea-level rise along the Atlantic Coast of the United States, *Geology*, *37*(12), 1115–1118.

Ezer, T., and L. P. Atkinson (2014), Accelerated flooding along the US East Coast: On the impact of sea-level rise, tides, storms, the Gulf Stream, and the North Atlantic Oscillations, *Earth's Future*, *2*(8), 362–382.

Ezer, T., and W. B. Corlett (2012), Is sea level rise accelerating in the Chesapeake Bay? A demonstration of a novel new approach for analyzing sea level data, *Geophys. Res. Lett.*, *39*, L19605, doi:10.1029/2012GL053435.

Ezer, T., L. P. Atkinson, W. B. Corlett, and J. L. Blanco (2013), Gulf Stream's induced sea level rise and variability along the US mid-Atlantic Coast, *J. Geophys. Res. Oceans*, *118*, 685–697.

Gehrels, W. R., G. A. Milne, J. R. Kirby, R. T. Patterson, and D. F. Belknap (2004), Late Holocene sea-level changes and isostatic crustal movements in Atlantic Canada, *Quat. Int.*, *120*(1), 79–89.

Ghosh, A., W. E. Holt, and L. M. Flesch (2009), Contribution of gravitational potential energy differences to the global stress field, *Geophys. J. Int.*, *179*, 787–81.

Hackl, M., R. Malservisi, U. Hugentobler, and R. Wonnacott (2011), Estimation of velocity uncertainties from GPS time series: Examples from the analysis of the South African TrigNet network, *J. Geophys. Res.*, *116*, B11404, doi:10.1029/2010JB008142.

Hayden, T., M. Kominz, D. S. Powars, L. E. Edwards, K. G. Miller, J. V. Browning, and A. A. Kulpecz (2008), Impact effects and regional tectonic insights: Backstripping the Chesapeake Bay impact structure, *Geology*, *36*(4), 327–330.

Hijma, M. P., S. E. Engelhart, T. E. Törnqvist, B. P. Horton, P. Hu, and D. F. Hill (2015), A protocol for a geological sea-level database, *Handb. Sea-Level Res.*, 536–553.

Horton, B. P., S. E. Engelhart, D. F. Hill, A. C. Kemp, D. Nikitina, K. G. Miller, and W. R. Peltier (2013), Influence of tidal-range change and sediment compaction on Holocene relative sea-level change in New Jersey, USA, *J. Quat. Sci.*, *28*(4), 403–411.

Karegar, M. A., T. H. Dixon, and R. Malservisi (2015), A three-dimensional surface velocity field for the Mississippi Delta: Implications for coastal restoration and flood potential, *Geology*, *43*(6), 519–522.

Karner, G. D. (1986), Effects of lithospheric in-plane stress on sedimentary basin stratigraphy, *Tectonics*, *5*(4), 573–588, doi:10.1029/TC005i004p00573.

Kemp, A. C., C. E. Bernhardt, B. P. Horton, R. E. Kopp, C. H. Vane, W. R. Peltier, A. D. Hawkes, J. P. Donnelly, A. C. Parnell, and N. Cahill (2014), Late Holocene sea-and land-level change on the US southeastern Atlantic Coast, *Mar. Geol.*, *357*, 90–100.
Kierulf, H. P., H. Steffen, M. J. R. Simpson, M. Lidberg, P. Wu, and H. Wang (2014), A GPS velocity field for Fennoscandia and a consistent comparison to glacial isostatic adjustment models, *J. Geophys. Res. Solid Earth*, *119*, 6613–6629.
Kominz, M. A., J. V. Browning, K. G. Miller, P. J. Sugarman, S. Mizintseva, and C. R. Scotese (2008), Late Cretaceous to Miocene sea-level estimates from the New Jersey and Delaware coastal plain coreholes: An error analysis, *Basin Res.*, *20*(2), 211–226.
Konikow, L. (2013), Groundwater depletion in the United States (1900–2008), *U.S. Geol. Surv. Sci. Invest. Rep., 2013-5079*.
Kooi, H., and J. J. De Vries (1998), Land subsidence and hydrodynamic compaction of sedimentary basins, *Hydrol. Earth Syst. Sci. Discuss.*, *2*(2/3), 159–171.
Kopp, R. E. (2013), Does the mid-Atlantic United States sea level acceleration hot spot reflect ocean dynamic variability?, *Geophys. Res. Lett.*, *40*, 3981–3985, doi:10.1002/grl.50781.
Lambeck, K., H. Rouby, A. Purcell, Y. Sun, and M. Sambridge (2014), Sea level and global ice volumes from the Last Glacial Maximum to the Holocene, *Proc. Natl. Acad. Sci. U.S.A.*, *111*(43), 15,296–15,303.
Mao, A., C. G. Harrison, and T. H. Dixon (1999), Noise in GPS coordinate time series, *J. Geophys. Res.*, *104*(B2), 2797–2816, doi:10.1029/1998JB900033.
Meng, A. A., and J. F. Harsh (1988), Hydrogeologic framework of the Virginia coastal plain, *U.S. Geol. Surv. Prof. Pap., 1404-C*.
Miller, K. G., R. E. Kopp, B. P. Horton, J. V. Browning, and A. C. Kemp (2013), A geological perspective on sea-level rise and its impacts along the US mid-Atlantic Coast, *Earth's Future*, *1*(1), 3–18.
Mitrovica, J. X., and G. A. Milne (2002), On the origin of late Holocene sea-level highstands within equatorial ocean basins, *Quat. Sci. Rev.*, *21*(20), 2179–2190.
Nikitina, D., A. C. Kemp, S. E. Engelhart, B. P. Horton, D. F. Hill, and R. E. Kopp (2015), Sea-level change and subsidence in the Delaware Estuary during the last ~ 2200 years, *Estuarine Coastal Shelf Sci.*, *164*, 506–519.
Park, K. D., R. S. Nerem, J. L. Davis, M. S. Schenewerk, G. A. Milne, and J. X. Mitrovica (2002), Investigation of glacial isostatic adjustment in the northeast US using GPS measurements, *Geophys. Res. Lett.*, *29*(11), 1509, doi:10.1029/2001GL013782.
Peltier, W. R. (2004), Global glacial isostasy and the surface of the ice-age Earth: The ICE-5G (VM2) model and GRACE, *Annu. Rev. Earth Planet. Sci.*, *32*, 111–149.
Peltier, W. R., and R. Drummond (2008), Rheological stratification of the lithosphere: A direct inference based upon the geodetically observed pattern of the glacial isostatic adjustment of the North American continent, *Geophys. Res. Lett.*, *35*, L16314, doi:10.1029/2008GL034586.
Peltier, W. R., D. F. Argus, and R. Drummond (2015), Space geodesy constrains ice age terminal deglaciation: The global ICE-6G_C (VM5a) model, *J. Geophys. Res. Solid Earth*, *120*, 450–487.
Rebischung, P., J. Griffiths, J. Ray, R. Schmid, X. Collilieux, and B. Garayt (2012), IGS08: The IGS realization of ITRF2008, *GPS Solution*, *16*(4), 483–494.
Rovere, A., P. J. Hearty, J. Austermann, J. X. Mitrovica, J. Gale, R. Moucha, A. M. Forte, and M. E. Raymo (2015), Mid-Pliocene shorelines of the US Atlantic coastal plain—An improved elevation database with comparison to Earth model predictions, *Earth Sci. Rev.*, *145*, 117–131.
Russo, T. A., A. T. Fisher, and B. S. Lockwood (2015), Assessment of managed aquifer recharge site suitability using a GIS and modeling, *Groundwater*, *53*(3), 389–400.
Sallenger, A. H., Jr., K. S. Doran, and P. A. Howd (2012), Hotspot of accelerated sea-level rise on the Atlantic Coast of North America, *Nat. Clim. Change*, *2*(12), 884–888.
Santamaría-Gómez, A., M. Gravelle, X. Collilieux, M. Guichard, B. M. Míguez, P. Tiphaneau, and G. Wöppelmann (2012), Mitigating the effects of vertical land motion in tide gauge records using a state-of-the-art GPS velocity field, *Global Planet. Change*, *98*, 6–17.
Sella, G. F., T. H. Dixon, and A. Mao (2002), REVEL: A model for recent plate velocities from space geodesy, *J. Geophys. Res.*, *107*(B4), 2081, doi:10.1029/2000JB000033.
Sella, G. F., S. Stein, T. H. Dixon, M. Craymer, T. S. James, S. Mazzotti, and R. K. Dokka (2007), Observation of glacial isostatic adjustment in stable North America with GPS, *Geophys. Res. Lett.*, *34*, L02306, doi:10.1029/2006GL027081.
Shennan, I., A. J. Long, and B. P. Horton (Eds.) (2015), *Handbook of Sea-Level Research*, John Wiley, Chichester, U. K.
Snay, R., M. Cline, W. Dillinger, R. Foote, S. Hilla, W. Kass, J. Ray, J. Rohde, G. Sella, and T. Soler (2007), Using global positioning system-derived crustal velocities to estimate rates of absolute sea level change from North American tide gauge records, *J. Geophys. Res.*, *112*, B04409, doi:10.1029/2006JB004606.
Trapp, H., and H. Meisler (1992), The regional aquifer system underlying the Northern Atlantic coastal plain in parts of North Carolina, Virginia, Maryland, Delaware, New Jersey, and New York: Summary, U.S. Geol. Surv. Prof. Pap., 1404-A,
Van De Plassche, O., A. J. Wright, B. P. Horton, S. E. Engelhart, A. C. Kemp, D. Mallinson, and R. E. Kopp (2014), Estimating tectonic uplift of the Cape Fear Arch (south-eastern United States) using reconstructions of Holocene relative sea level, *J. Quat. Sci.*, *29*(8), 749–759.
Williams, S. D. (2008), CATS: GPS coordinate time series analysis software, *GPS Solutions*, *12*(2), 147–153.
Yang, Q., T. H. Dixon, P. G. Myers, J. Bonin, D. Chambers, and M. R. van den Broeke (2016), Recent increases in Arctic freshwater flux: Impacts on Labrador Sea Convection and Atlantic overturning circulation, *Nat. Commun.*, *7*, 10525, doi:10.1038/ncomms10525.
Zoback, M. L. (1992), Stress field constraints on intraplate seismicity in eastern North America, *J. Geophys. Res.*, *97*(B8), 11,761–11,782, doi:10.1029/92JB00221.